

Drug Repurposing Hypothesis Validation with Knowledge-infused Explanations

Susana Nunes^{1,*}, Catia Pesquita¹

¹LASIGE, Faculty of Sciences, University of Lisbon, Lisbon, Portugal

Abstract

As the need for effective and swiftly deployable medications grows, drug repurposing has become a pivotal strategy to mitigate the traditionally long and costly drug development process. Artificial Intelligence (AI), primarily through deep learning, is revolutionizing drug discovery by identifying novel uses for existing drugs, thus expediting therapeutic breakthroughs. Despite these advancements, the complexity of these models and their unknown internal workings pose significant challenges in understanding and trusting their predictions.

This paper introduces a novel method for knowledge-driven explanations of drug repurposing AI-based predictions, that focuses on scientific validation. The method uses Knowledge Graph technologies to provide transparent, knowledge-infused explanations of AI-derived predictions. The integration of biomedical ontologies elucidates the biological mechanisms underlying these predictions, aiming to enhance human comprehension and trust in AI applications.

We applied our method to Hetionet, an integrated network comprising 29 leading biomedical databases, which we further enriched with two biomedical ontologies NCIT and CHEBI. The explanations generated by our method are consistent with ground truth drug repurposing mechanisms, and illustrate the crucial role that ontologies can have in enriching scientific knowledge-infused explanations.

Keywords

Explainable Artificial Intelligence, Drug Repurposing, Biomedical Knowledge Graphs, Logical Reasoning

1. Introduction

The global demand for safe and efficient medications is escalating due to an aging population and a better understanding of disease burdens. However, the current process of bringing a new drug to market averages 14 years and costs around US\$3 billion. With expenses soaring and failure rates high, researchers are seeking ways to streamline drug discovery and development using artificial intelligence (AI). AI, in particular through deep learning, has become integral to therapeutic discovery, offering a means to generate actionable predictions for laboratory testing. AI tools are aiding in the discovery of new antibacterial drugs, accurately predicting protein structures, and identifying drug repurposing opportunities, whereby new therapeutic targets are discovered for existing drugs [1, 2, 2]. Many recent and well-established companies in the field of drug discovery have secured substantial funding over the past few years. Their business strategies predominantly hinge on integrating advanced physics-based molecular modeling alongside deep learning (DL) and AI technologies [3].

Still, there are standing challenges in drug discovery with AI. In fact, the AstraZeneca-Sanger Cancer Drug Combination Prediction DREAM Challenge [4] – a competition for ML in drug synergy – observed that the ML method itself had little impact on overall performance but that it is essential that modelling approaches reveal testable biological insight – a conclusion that translates to all drug discovery tasks. Explainable AI (XAI) in drug discovery is a theme that is fast gaining attention [5].

Drug repurposing predictions, including those generated by black-box methods, can be construed as scientific hypotheses that require lab experiments and clinical trials to be validated. However, 90% of clinical trials fail [6]; therefore, a computational validation of these hypotheses to identify the most promising candidates would improve outcomes in pre-clinical and clinical studies, leading to the

DAO-XAI 2024: Workshop on Data meets Applied Ontologies in Explainable AI, October 19, 2024, Santiago de Compostela, Spain
*Corresponding author.

 scnunes@ciencias.ulisboa.pt (S. Nunes); clpesquita@ciencias.ulisboa.pt (C. Pesquita)

 0000-0002-0160-5875 (S. Nunes); 0000-0002-1847-9393 (C. Pesquita)



© 2024 Copyright for this paper by its authors. Use permitted under Creative Commons License Attribution 4.0 International (CC BY 4.0).

development of more effective, accessible, and safer medications. The computational validation of these hypotheses would require checking how the prediction fits with existing scientific knowledge.

In this paper, we present a method to generate explanations to support knowledge-driven validation of scientific hypotheses, and apply it for drug repurposing.

2. Motivation

AI systems can predict potential drug repurposing opportunities by analyzing extensive biomedical datasets and utilizing sophisticated algorithmic models [7]. This enables the identification of existing drugs that may be effective for new therapeutic applications, supporting innovative treatment strategies. To achieve this, AI systems use various mining methods, such as vector-based approaches, machine learning algorithms, deep learning algorithms, or basic language models [1, 2, 8].

Although AI systems are effective, a major concern is that they can be opaque boxes with unknown or incomprehensible internal mechanisms to humans [9]. Validating AI's black-box predictions against existing knowledge ensures they are medically sound and not just technically accurate. This step is crucial for building trust and achieving approval by confirming that predictions align with known scientific and medical principles. Accordingly, XAI aims to enhance trust in AI systems and enable informed decision-making by increasing transparency and interpretability of AI algorithms [10].

XAI methods vary in how they generate explanations, with many focusing on improving model interpretability by identifying key features and weights that influence predictions. While data-based approaches are common, they often analyze input data without incorporating external information, such as prior knowledge [11]. This can limit their ability to provide the necessary semantic context, making it harder for humans to understand and trust AI outcomes. These approaches offer insights into the operations of black-box AI models but might not fully explain how these models arrive at their conclusions.

More recently, Explainable Knowledge-enabled Systems have been proposed as a potential solution by incorporating domain knowledge to generate context-sensitive explanations that are comprehensible to the user and equipped with provenance information [12]. This highlights the need to integrate a representation of established domain knowledge into AI systems for specific fields. The use of Semantic Web technologies, such as ontologies and knowledge graphs (KGs), can potentially address the issue of knowledge-infused explanations, as they offer the required semantic context to data [13]. Knowledge-infused Explanations integrate domain-specific knowledge or external information sources into machine-learning model descriptions to better understand the model's reasoning [14]. For instance, in drug repurposing systems, explanations might highlight how certain molecular interactions or genetic markers influence the likelihood of a drug being effective for a new therapeutic use, rather than merely listing all considered data. However, current approaches that use ontologies and KGs for XAI are still in their early stages and mostly fail to capture the importance of features and the rationale behind their relevance given a context.

3. Related Work

Incorporating these insights, recent works have advanced the use of KGs and AI techniques in drug repurposing. Liu et al. [15] presents PoLo, a neuro-symbolic approach that combines representation learning with logic to enhance drug repurposing efforts and provide interpretable reasoning paths.

The PoLo (Policy-guided Logical Reasoning) method operates by integrating two main components:

- Policy-guided walks with reinforcement learning: This component uses reinforcement learning to navigate KGs, helping to discover significant paths between entities like drugs and diseases based on learned policies.
- Logical rules for reward shaping: Logical rules are integrated into the reward function, ensuring that the discovered paths are not only statistically significant but also logically coherent, thus enhancing interpretability.

By combining these elements, PoLo predicts new drug-disease relationships and provides clear explanations for these predictions. The use of logical rules ensures the model’s interpretability, addressing a critical challenge in AI-driven drug repurposing. Liu et al. [15] applied PoLo to Hetionet, and their results indicated that PoLo outperformed several methods for link prediction, demonstrating its potential in drug repurposing applications.

Similarly, Stork et al. [16] developed a method to improve the quality of explanatory paths in drug repurposing, integrating contextual knowledge with a reinforcement learning-based approach. Moreover, Ozkan et al. [17] extends the PREDICT method [18] with a knowledge graph-based approach that identifies and ranks paths within a KG that elucidate drug indications, drawing on similarities to established drug-disease relationships.

4. Methods

4.1. Overview

Our method generates explanations for individual drug repurposing predictions. We define a drug repurposing prediction as a tuple $\langle dr, di \rangle$ where dr is a drug and di is a disease. The intuition behind our method is that by mapping drugs and diseases to a KG that describes biomedical entities, relevant paths may be found between drugs and diseases that can contextualize the prediction in existing scientific knowledge. Let’s take as an example the most famous case of drug repurposing: aspirin. Originally used for pain relief and as an anti-inflammatory, aspirin has since been widely used in a variety of clinical settings to manage numerous diseases [19], including its repurposing for anticoagulant properties to prevent blood clots, thereby reducing the risk of heart attacks and strokes. Using our method, we could map aspirin and cardiovascular diseases to a biomedical KG. This KG might reveal pathways connecting aspirin to processes involved in blood clotting and inflammation, providing a scientific basis for understanding how aspirin helps in the prevention of cardiovascular events.

Moreover, the size of an explanation is also a crucial requirement driven by the limitations of human cognitive capacity. Explanations should be concise, brief, and free of redundancy to prevent them from being too large to comprehend [20], more concise paths, preferably within the length of 5 to 7 nodes, while still maintaining relevance. This strategy is based on the understanding that humans can hold between around 7 objects in short-term memory [21]. Therefore, our method focuses on identifying shorter, yet relevant, paths within the KG to enhance the interpretability and practical application of the drug repurposing predictions. The overall method is outlined in Figure 1A.

We define an explanation for a drug repurposing prediction $\langle dr, di \rangle$ as a subset of paths P within the knowledge graph KG that link the drug dr to the disease di .

Formally, an explanation E for the prediction $\langle dr, di \rangle$ can be expressed as:

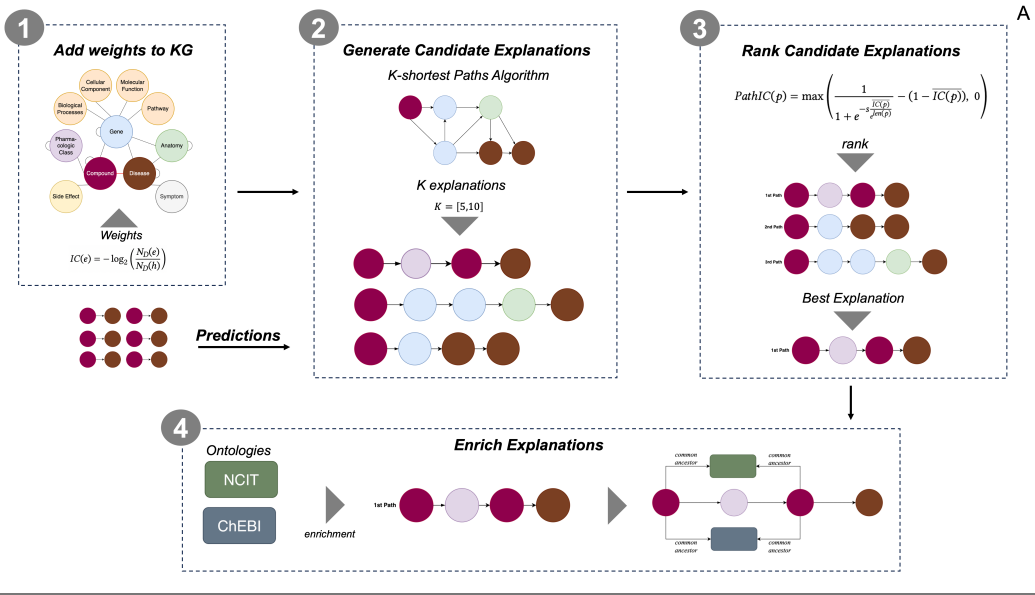
$$E(dr, di) = \arg \max_{p \in P_{dr \rightarrow di}} \{PathIC(p)\} \quad (1)$$

where $P_{dr \rightarrow di}$ is the set of k-shortest paths in the KG linking dr and di and $PathIC$ is a measure of the informativeness of the path that we want to maximize.

Given a KG that includes drugs and diseases, and a given drug repurposing prediction we aim to explain, the first step is to *Add weights to the KG* to reflect the informativeness of each node in the KG. This weighting helps prioritize more informative paths.

In the second step *Generate Candidate Explanations*, our method considers between 5 and 10 candidates. This range is chosen to balance computational efficiency and explanation quality. Too few candidates might miss relevant pathways, while too many can introduce noise, complicating the extraction of valuable conclusions. Limiting to 5-10 candidates ensures a manageable and high-quality set for evaluation. These candidates are found through a k-shortest paths algorithm, which identifies the top k paths from the source to the target within a KG. This algorithm ensures that the most relevant and diverse paths are selected by considering the edge weights, thereby generating a comprehensive set of potential core paths. Following the candidate generation, these core paths are evaluated and ranked to

Generating Explanations



Evaluation

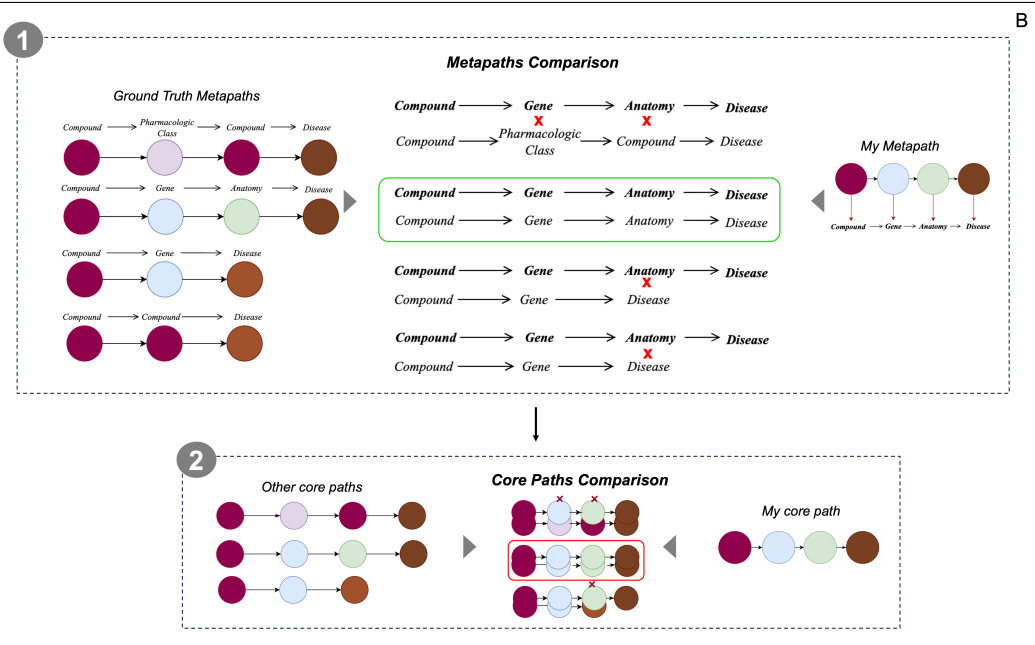


Figure 1: Overview of our method to generate candidate explanations, rank them, and enrich them (A) and its evaluation strategy (B).

find the best-suited explanations for each prediction. The core paths are also extended to enrich the explanations by incorporating neighborhood information using ontologies.

4.2. Add Weights to the KG

To add weights to the edges of the KG we explored the concept of Information Content (IC), a measure of how specific and informative a concept is, and takes advantage of KG properties, such as node degree counts. The degree of the node is the number of edges (relations) connected to the node (entity). To determine the informativeness of a path, the approach first calculates a normalized node IC for each entity, which is given by:

$$IC(e) = -\log_2 \left(\frac{N_D(e)}{N_D(h)} \right) \quad (2)$$

where $N_D(e)$ is the node degree of the entity e , and $N_D(h)$ is the node degree of the entity h with the highest node degree of all entities.

4.3. Generate Explanations

4.3.1. Generate Candidate Explanations

In order to obtain candidate explanations, we employed a k-shortest path algorithm based on Yen [22] work. While the algorithm presumed the use of the Dijkstra algorithm [23] for identifying the shortest path between two nodes, the method can incorporate any shortest path-finding algorithm as a substitute. We used the NetworkX¹ library for the implementation, a powerful tool for studying graphs and networks. NetworkX offers a comprehensive range of algorithms designed for graph analysis, allowing us to implement and execute Yen's algorithm efficiently within our method.

4.3.2. Rank Candidate Explanations

After gathering candidate explanations, we rank them to identify the most relevant one.

To do this step, we take advantage of the node-specific properties of the IC measure, and a second measure emerges to calculate the information level of the path.

The Path IC is a sigmoid defined as follows:

$$PathIC(p) = \max \left(\frac{1}{1 + e^{-s \frac{\overline{IC}(p)}{e^{len(p)}}}} - (1 - \overline{IC}(p)), 0 \right) \quad (3)$$

The parameters s and p play a crucial role in adjusting the sensitivity of the function to changes in the IC over the nodes in a path. Specifically,

- $s = 300$, acts as a scaling factor to amplify the exponential function's argument within the sigmoid function. This choice of s ensures that the function is highly responsive to variations in the ratio between $\overline{IC}(p)$ and $e^{len(p)}$, allowing for a fine-tuned adjustment of the function's behavior.
- $len(p)$, the length of path p is determined by the total count of nodes present in a given path, thereby directly incorporating the path length into our calculation. This allows us to account for the length of the path in a straightforward manner, adjusting the average IC with an exponential decay factor, $\exp(len(p))$, to ensure a calibrated evaluation of longer paths.
- $\overline{IC}(p)$ is the average IC of all nodes in the path.

$PathIC$ is designed to penalize longer paths. In Figure 2, the function's curve reveals how the measure discourages overly long paths. It starts with a high value for short paths, indicating a minimal penalty. As the paths become longer, the value quickly decreases, showing a significant penalty for increasing path length. However, the curve begins to flatten beyond a certain point, indicating that while the model penalizes longer paths, after a certain length, the penalty rate lessens. The different IC curves illustrate that although paths with higher average IC values are initially preferred, the path choice does not always favor those with the highest average IC as the path length increases. For example, a path of length 6 with an average IC of 0.8 ranks below a path of length 4 with an average IC of 0.6. However, the model might select longer paths with higher average IC values when the penalty for additional length becomes minimal. This balance ensures that the chosen paths are optimal, considering both length and IC value.

¹<https://networkx.org/>

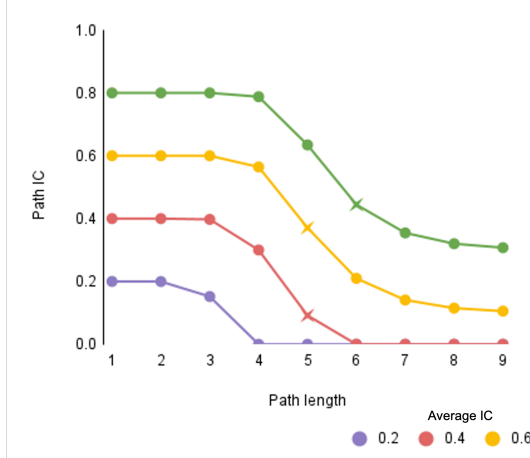


Figure 2: Distribution graph of the IC penalization according to each path length given the sigmoid function for different average IC.

4.3.3. Enrich explanations

After assessing the relevant core paths, we enrich the explanations by incorporating neighborhood information using ontologies. Specifically, we employed the NCIT (National Cancer Institute Thesaurus) [24] and ChEBI (Chemical Entities of Biological Interest) [25] ontologies to enhance the contextual understanding of the relationships between entities. This enrichment involved exploring related entities and their hierarchical relationships within the ontologies. By leveraging the structured knowledge within NCIT and ChEBI, we were able to find the lowest common ancestors between the entities in the path. These common ancestors represent higher-level classes that connect the entities through shared parents (*subclass of* relations).

4.4. Evaluation approach

The evaluation method (Figure 1B) focuses on validating the generated explanations. It assesses the consistency of the explanations by aligning the generated metapaths with established ground truths and comparing core paths to other approaches.

A metapath is defined as a sequence of entity types and relationships in the KG that represents a generalized relation between entities. Formally, a metapath can be represented as a tuple $\langle E_1, r_1, E_2, r_2, \dots, E_n \rangle$ where E_i are entity types and r_i are relationship types in the KG.

Looking into more concrete example, if we want to represent a relation between a given drug and disease. A core path can represent a detailed path from Mitomycin to Stomach Cancer, delineating the explicit relationships and entities involved.

$$\text{Mitomycin} \xrightarrow{\text{downregulates}} \text{TNFSF9 Gene} \xleftarrow{\text{associates}} \text{Stomach Cancer}$$

Contrarily in a metapath, instead of detailing Mitomycin's interaction with a particular gene and cancer, the metapath only reveals the pattern.

$$\text{Compound} \xrightarrow{\text{downregulates}} \text{Gene} \xleftarrow{\text{associates}} \text{Disease}$$

We performed an ablation study in our experimental design were our method (WG-S) was evaluated against three variations according to the different criteria used to generate the explanations:

- The full method **WG-S**: generates explanations considering weights in the KG and ranks them using the Path IC;
- The **WG-A** variant: calculates a different Path(IC) through an average IC of the nodes in the core explanation path, allowing the investigation of the impact of modulating explanation length;

- The **NWG-S** variant: does not consider KG weights;
- The **NWG-A** variant: does not consider weights and employs a different Path IC with an average for ranking.

4.5. Application to Hetionet

In the realm of biomedical research, the integration of diverse datasets is crucial for uncovering novel insights and therapeutic opportunities. To validate and demonstrate our method, we applied it to Hetionet [26], a comprehensive biomedical KG. Hetionet aggregates biomedical information from 29 distinct databases into a unified network. It encompasses data spanning over five decades, including compounds and diseases. This comprehensive resource features 47,031 nodes of 11 different types and 2,250,197 relationships across 24 categories (Figure 3). By integrating diverse biomedical datasets, Hetionet facilitates the generation of new hypotheses and insights, offering a holistic platform for exploring data across various domains.

For a drug repurposing study, Hetionet’s comprehensive database includes 1,552 compounds and 137 diseases, interconnected through 775 documented *treats* associations. Adopting the dataset partitioning strategy outlined in the PoLo method [15], the 775 triples were divided into distinct sets: 483 triples for the training set, 121 triples for the validation set, and 151 triples for the test set, where the latter set was used for evaluation.

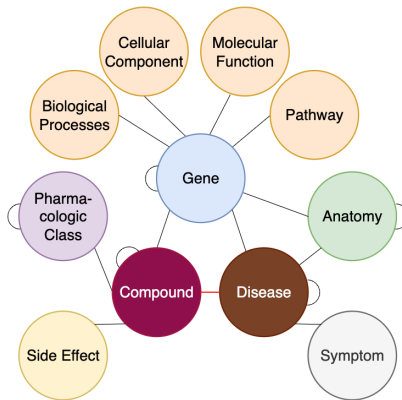


Figure 3: Hetionet [26] comprises a schema that features 11 types of entities and unique relation types that interconnect them. The relation of interest for drug repurposing is highlighted in red.

4.5.1. Metapaths Comparison

For the Metapaths Comparison aspect of our evaluation, we define our ground truth using a refined approach inspired by the findings of Himmelstein et al. [26], who examined 1206 metapaths connecting *Compound* and *Disease* entities to uncover various mechanisms of pharmacological efficacy. They identified 27 metapaths with significant predictive power for drug efficacy, using them as features in a logistic regression model to calculate the probability of a compound treating a disease. Building on their groundwork, we selected 14 of these metapaths based on their detection by our method. We adopt these 14 metapaths as our ground truth, as shown in Table 1.

This evaluation intends to assess the consistency of our explanations against the established ground truth. This comparison helps us determine how well our identified metapaths align with those recognized as noteworthy in predicting drug efficacy. Through this process, we aim to validate the robustness and informativeness of our explanations, ensuring they are structurally sound in the context of existing scientific knowledge.

Besides using the ground truth, we additionally compare our metapaths with PoLo to measure the alignment of our findings. We seek to understand how our method correlates with their method in an

Table 1

Ground Truth metapaths used for evaluation.

Path	Ground Truth
1	<i>Compound</i> $\xleftarrow{\text{includes}}$ <i>PharmacologicClass</i> $\xrightarrow{\text{includes}}$ <i>Compound</i> $\xrightarrow{\text{treats}}$ <i>Disease</i>
2	<i>Compound</i> $\xrightarrow{\text{resembles}}$ <i>Compound</i> $\xrightarrow{\text{resembles}}$ <i>Compound</i> $\xrightarrow{\text{treats}}$ <i>Disease</i>
3	<i>Compound</i> $\xrightarrow{\text{binds}}$ <i>Gene</i> $\xleftarrow{\text{associates}}$ <i>Disease</i>
4	<i>Compound</i> $\xrightarrow{\text{resembles}}$ <i>Compound</i> $\xrightarrow{\text{treats}}$ <i>Disease</i>
5	<i>Compound</i> $\xrightarrow{\text{palliates}}$ <i>Disease</i> $\xleftarrow{\text{palliates}}$ <i>Compound</i> $\xrightarrow{\text{treats}}$ <i>Disease</i>
6	<i>Compound</i> $\xrightarrow{\text{binds}}$ <i>Gene</i> $\xleftarrow{\text{binds}}$ <i>Compound</i> $\xrightarrow{\text{treats}}$ <i>Disease</i>
7	<i>Compound</i> $\xrightarrow{\text{causes}}$ <i>SideEffect</i> $\xleftarrow{\text{causes}}$ <i>Compound</i> $\xrightarrow{\text{treats}}$ <i>Disease</i>
8	<i>Compound</i> $\xrightarrow{\text{treats}}$ <i>Disease</i> $\xrightarrow{\text{resembles}}$ <i>Disease</i>
9	<i>Compound</i> $\xrightarrow{\text{resembles}}$ <i>Compound</i> $\xrightarrow{\text{binds}}$ <i>Gene</i> $\xleftarrow{\text{associates}}$ <i>Disease</i>
10	<i>Compound</i> $\xrightarrow{\text{binds}}$ <i>Gene</i> $\xleftarrow{\text{expresses}}$ <i>Anatomy</i> $\xleftarrow{\text{localizes}}$ <i>Disease</i>
11	<i>Compound</i> $\xrightarrow{\text{downregulates}}$ <i>Gene</i> $\xleftarrow{\text{upregulates}}$ <i>Disease</i>
12	<i>Compound</i> $\xrightarrow{\text{upregulates}}$ <i>Gene</i> $\xleftarrow{\text{downregulates}}$ <i>Disease</i>
13	<i>Compound</i> $\xrightarrow{\text{treats}}$ <i>Disease</i> $\xleftarrow{\text{localizes}}$ <i>Anatomy</i> $\xleftarrow{\text{localizes}}$ <i>Disease</i>
14	<i>Compound</i> $\xrightarrow{\text{treats}}$ <i>Disease</i> $\xrightarrow{\text{presents}}$ <i>Symptom</i> $\xleftarrow{\text{presents}}$ <i>Disease</i>

explainable perspective.

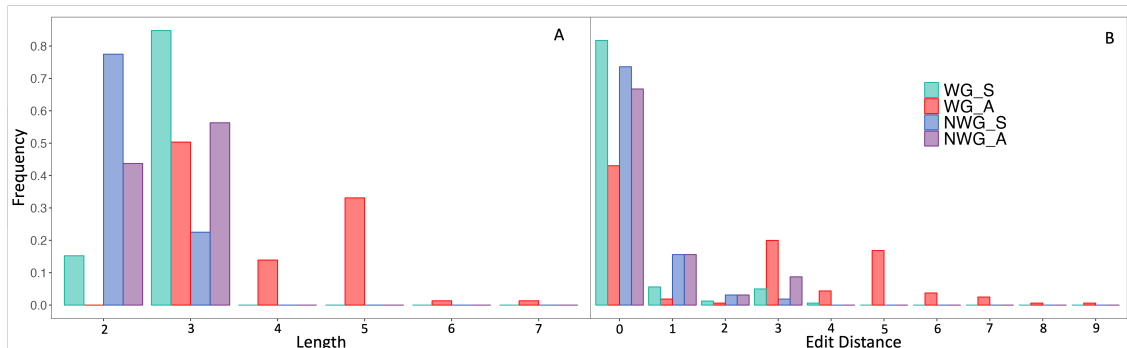
4.5.2. Core Paths Comparison

For the Core Paths Comparison, we aimed to understand how closely our explanations align with those identified in PoLo. We were particularly interested in whether our findings match theirs and, if not, whether the information content of the paths significantly influences these differences. This approach helps us assess the depth of our model and understand how the IC measure affects the selection of explanations.

5. Results and Discussion

In this section, we present and analyze our method's results, highlighting the performance of the different variants and discussing their implications. We aim to provide a comprehensive understanding of how each variant influences the generation and selection of candidate explanations and how these choices impact the overall effectiveness of our approach.

Starting by analyzing the path length frequency among methods variations in Figure 4A, they generally favor path lengths between 2 and 3.

**Figure 4:** Explanations frequency of length (A) and edit distance (B) for each variant.

However, variants using the sigmoid function (WG-S and NWG-S) demonstrate a preference for moderately short paths, reflecting the function's tendency to penalize longer paths more heavily. In contrast, those using the average function (WG-A and NWG-A) present a broader distribution, indicating a less selective path evaluation. Moreover, the use of weights in WG-S and WG-A allows for a more detailed consideration of path components, enhancing the selection process based on the informativeness of connections within the KG. Conversely, NWG-S and NWG-A, which do not use weights, adopt a simpler, more uniform approach, focusing primarily on path length.

5.1. Meta paths-based analysis

We performed two analyses based on meta paths extracted for our explanations: a comparison to the paths identified in [26] as relevant for drug-repurposing (*ground truth*) and a comparison to the metapaths extracted from PoLo's explanations.

5.1.1. Ground truth-based analysis

When evaluating the structure of our metapaths against ground truth, we measured the differences through the concept of *edit distance*. An *edit distance* quantifies the number of single-element changes (additions, deletions, or substitutions of nodes and edges) required to transform the predicted metapath into the ground truth path. An edit distance of zero means the predicted metapath exactly matches the ground truth without any discrepancies. Figure 4B shows a plot based on the frequency of edit distances required by each variant to align with a ground truth path.

Results show WG-S and NWG-S with several metapaths that align perfectly with a ground truth path without any intermediary modifications (0 edit distances). This suggests a strong alignment with the ground truth and highlights the effectiveness of the sigmoid function in these variants, which inherently favors shorter paths and leads the explanation towards ranking as the best path, a more direct path between the compound and disease.

We can also see that WG-A exhibits a varied distribution of edit distances, suggesting its predictions span a wide range of path modifications. In contrast, NWG-A demonstrates a more consistent pattern of edit distances, and upon looking into the explanations generated, it showed a tendency towards fewer modifications. This difference highlights the impact of KG weights when retrieving candidate explanations. WG-A considers each edge's informativeness, leading to a broader spectrum of edit distances. Contrarily, without the influence of weights, NWG-A may default to the shortest possible path, disregarding the informativeness of the paths identified. This shows how the presence or absence of weights can significantly shape the variant's approach to identifying the best path between nodes.

Table 2 further clarifies the distinct behaviors of the four variants in the choice of ground truth path without any edit distance necessary.

We can observe the WG-S and WG-A variant show a preference for paths, such as Path7, which involves the causality between a compound's side effects in common and its therapeutic application. In contrast, variants NWG-S and NWG-A manifest an ability to generate simpler paths, such as Path3, where the compound-gene-disease relationship follows a more short and direct pattern. However, it seems less effective in more complex paths where additional biological context provided by weights may be beneficial.

Regarding the metapaths that did not align with the established ground truth, Table 3 presents alternative paths generated by the WG-S, which could nonetheless hold relevance. Such paths may represent underexplored yet biologically meaningful interactions that could lead to new hypotheses validation in drug repurposing predictions.

5.1.2. Comparison with PoLo's metapaths

Regarding the comparison with PoLo's metapaths, PoLo explained only 115 out of 151 predictions. The subsequent analysis will focus on these explained paths. Figure 5A shows how the frequency of metapaths of our method and variants aligns with PoLo's. We can observe a higher alignment with

Table 2

Frequency of paths aligned with the ground truth.

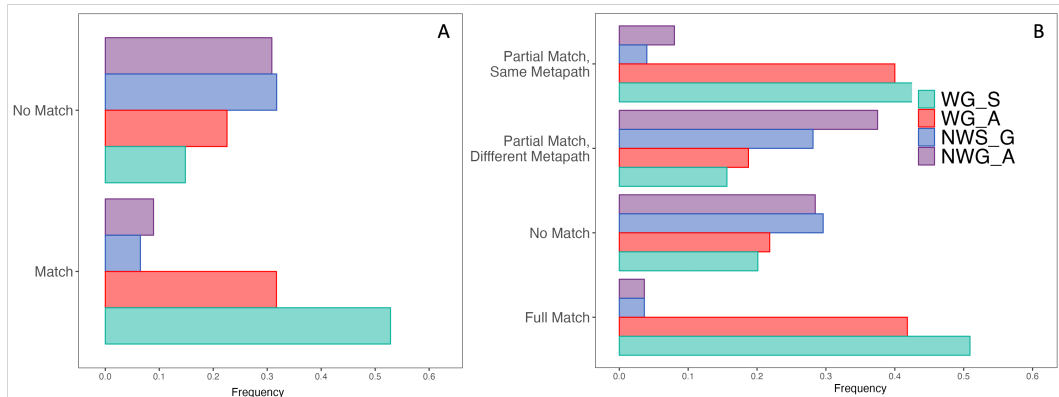
Path Frequency	WG-S	WG-A	NWG-S	NWG-A
Path 1	26	15	0	0
Path 2	1	1	0	5
Path 3	10	0	46	22
Path 4	3	0	27	16
Path 5	0	0	0	0
Path 6	3	1	1	4
Path 7	59	35	16	26
Path 8	0	0	14	4
Path 9	2	0	1	3
Path 10	1	1	1	5
Path 11	1	0	0	0
Path 12	3	0	4	3
Path 13	6	7	2	6
Path 14	16	9	6	13

Table 3

Explanations that did not fully align with the ground truth, using WG-S.

		Paths
1	<i>Compound</i>	$\xrightarrow{\text{causes}} \text{SideEffect} \xleftarrow{\text{causes}} \text{Compound} \xrightarrow{\text{palliates}} \text{Disease}$
2	<i>Compound</i>	$\xrightarrow{\text{upregulates}} \text{Gene} \xleftarrow{\text{associates}} \text{Disease}$
3	<i>Compound</i>	$\xleftarrow{\text{includes}} \text{PharmacologicClass} \xrightarrow{\text{includes}} \text{Compound} \xrightarrow{\text{palliates}} \text{Disease}$
4	<i>Compound</i>	$\xrightarrow{\text{resembles}} \text{Compound} \xrightarrow{\text{binds}} \text{Gene} \xleftarrow{\text{associates}} \text{Disease}$
5	<i>Compound</i>	$\xrightarrow{\text{upregulates}} \text{Gene} \xleftarrow{\text{upregulates}} \text{Disease}$
6	<i>Compound</i>	$\xrightarrow{\text{palliates}} \text{Disease} \xrightarrow{\text{presents}} \text{Symptom} \xleftarrow{\text{presents}} \text{Disease}$
7	<i>Compound</i>	$\xrightarrow{\text{palliates}} \text{Disease} \xrightarrow{\text{localizes}} \text{Anatomy} \xleftarrow{\text{localizes}} \text{Disease}$
8	<i>Compound</i>	$\xrightarrow{\text{binds}} \text{Gene} \xleftarrow{\text{covaries}} \text{Gene} \xleftarrow{\text{associates}} \text{Disease}$
9	<i>Compound</i>	$\xrightarrow{\text{upregulates}} \text{Gene} \xrightarrow{\text{regulates}} \text{Gene} \xleftarrow{\text{downregulates}} \text{Disease}$

both weighted variants. Specifically, WG-S shows the highest agreement with PoLo. On the other hand, variants that do not consider weights tend to diverge significantly from the PoLo method, which may emphasize the importance of weights in achieving more relevant paths instead of aspiring for shorter paths.

**Figure 5:** Frequency of alignment between PoLo metapaths and each variant's metapaths (A) and PoLo core paths with each variant's core paths (B).

5.2. Explanation analysis

Regarding the core paths comparison step, Figure 5B presents the frequency of core paths from our method and variants aligning with PoLo's.

Notably, the weighted variants exhibit a higher number of complete entity matches, just like in the metapaths, suggesting a more substantial alignment with PoLo's core paths than other variants. Nevertheless, the main overlaps exist in the *No Match* row.

We computed the average IC for each path generated both by our variants and PoLo method (Figure 6). Our main approach has a distribution very close to PoLo's, while the non-weighted variants had lower average IC scores. We compared the distributions of the average ICs using the Kruskal-Wallis test, followed by pairwise comparisons with Dunn's test and Bonferroni adjustment for multiple comparisons with $p < 0.01$. The test revealed that PoLo and WG-S are not significantly different but that all other methods differ significantly between themselves.

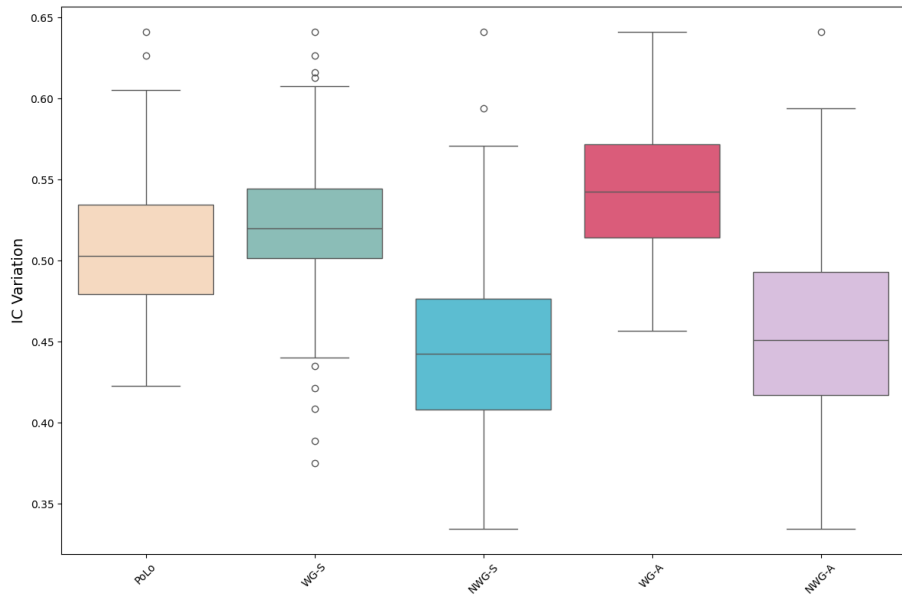


Figure 6: IC distribution for PoLo and each variant.

5.3. Use case examples

Besides evaluating the core paths we enriched them with the ontologies NCIT and CHEBI. Figure 7 present examples of enriched paths for a given predicted repurposing.

In Figure 7a, the path illustrates the potential repurposing of Aminophylline for Chronic Obstructive Pulmonary Disease (COPD). The core path shows that Aminophylline treats asthma, which presents dyspnea paroxysmal, a symptom also present in COPD. The path is enriched by linking these entities to a common ancestor, Chronic Lung Disorder, providing a broader context and biological relevance. This enrichment highlights the shared symptomatic and disease mechanisms between asthma and COPD, justifying the repurposing prediction.

In Figure 7b, the path illustrates the potential repurposing of Vinorelbine for Breast Cancer treatment. The core path connects Vinorelbine's binding action on the TUBB8 gene to Eribulin, another compound that also binds TUBB8 and is used to treat breast cancer. The enrichment involves linking these compounds and their actions to broader categories such as Organo-nitrogen Compound and Vinca-Domain Binding Agent. This enriched path provides a detailed view of how these compounds may interact with the gene. The connection to the Vinca-Domain Binding Agent is validated by literature indicating that Vinca-domain ligands are a class of microtubule inhibitors with great potential for

cancer therapy [27]. This supports the explanation and further justifies the repurposing potential of Vinorelbine for breast cancer treatment

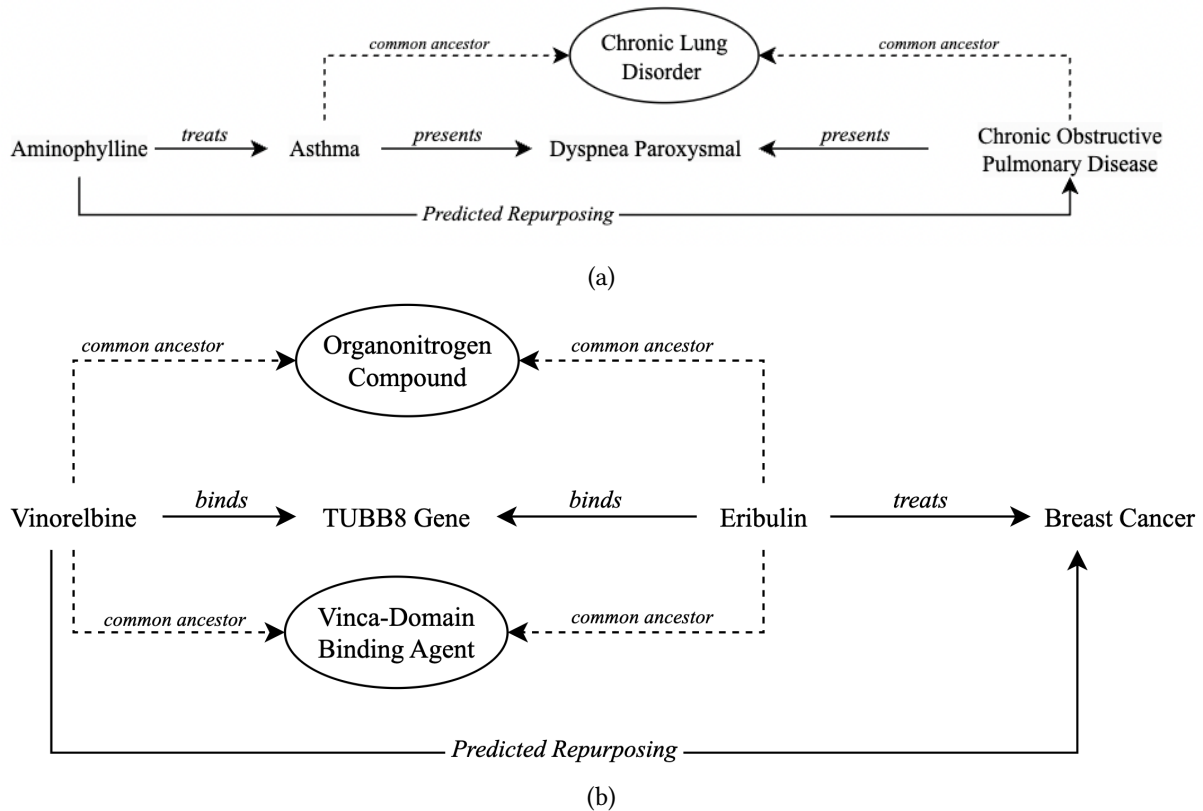


Figure 7: Enriched paths between (A) Aminophylline and Chronic Obstructive Pulmonary Disease, (B) Vinorelbine and Breast Cancer

6. Conclusions

To accelerate therapeutics innovation by unlocking the potential of Explainable AI in the realm of drug repurposing, we present a novel method of generating explanations. It addresses the critical need for transparency and understanding in AI-driven predictions by effectively integrating biomedical knowledge into the validation process. This integration allows for deeper scrutiny and justification of AI-generated hypotheses with black-box neural methods, ensuring that each prediction aligns with and is reinforced by established scientific knowledge.

We applied our method to Hetionet, and results showed a high rate of exact metapath matches, confirming the method's effectiveness in providing clear, scientifically valid explanations. This preliminary work represents a crucial first step toward offering scientific explanations for drug repurposing predictions. Eventually, this approach aims to fulfill the objective of enhancing AI's trustworthiness by paving the way for future studies, including user studies with clinicians, to further validate and improve the practical application of AI in drug repurposing.

Acknowledgments

This work was supported by FCT through the fellowship 2023.00653.BD and through the LASIGE Research Unit, ref. UIDB/00408/2020 (<https://doi.org/10.54499/UIDB/00408/2020>) and ref. UIDP/00408/2020 (<https://doi.org/10.54499/UIDP/00408/2020>). It was also partially supported by the KATY project which

has received funding from the European Union's Horizon 2020 research and innovation program under grant agreement No 101017453.

References

- [1] F. Napolitano, D. Carrella, B. Mandriani, S. Pisonero-Vaquero, F. Sirci, D. L. Medina, N. Brunetti-Pierri, D. Di Bernardo, gene2drug: a computational tool for pathway-based rational drug repositioning, *Bioinformatics* 34 (2018) 1498–1505.
- [2] A. Zhavoronkov, Y. A. Ivanenkov, A. Aliper, M. S. Veselov, V. A. Aladinskiy, A. V. Aladinskaya, V. A. Terentiev, D. A. Polykovskiy, M. D. Kuznetsov, A. Asadulaev, et al., Deep learning enables rapid identification of potent ddr1 kinase inhibitors, *Nature biotechnology* 37 (2019) 1038–1040.
- [3] A. V. Sadybekov, V. Katritch, Computational approaches streamlining drug discovery, *Nature* 616 (2023) 673–685.
- [4] M. P. Menden, D. Wang, M. J. Mason, B. Szalai, K. C. Bulusu, Y. Guan, T. Yu, J. Kang, M. Jeon, R. Wolfinger, et al., Community assessment to advance computational prediction of cancer drug combinations in a pharmacogenomic screen, *Nature communications* 10 (2019) 2674.
- [5] J. Jiménez-Luna, F. Grisoni, G. Schneider, Drug discovery with explainable artificial intelligence, *Nature Machine Intelligence* 2 (2020) 573–584.
- [6] D. Sun, W. Gao, H. Hu, S. Zhou, Why 90% of clinical drug development fails and how to improve it?, *Acta Pharmaceutica Sinica B* 12 (2022) 3049–3062.
- [7] R. Amiri, J. Razmara, S. Parvizpour, H. Izadkhah, A novel efficient drug repurposing framework through drug-disease association data integration using convolutional neural networks, *BMC bioinformatics* 24 (2023) 442.
- [8] F. Yang, Q. Zhang, X. Ji, Y. Zhang, W. Li, S. Peng, F. Xue, Machine learning applications in drug repurposing, *Interdisciplinary Sciences: Computational Life Sciences* 14 (2022) 15–21.
- [9] R. Goebel, A. Chander, K. Holzinger, F. Lecue, Z. Akata, S. Stumpf, P. Kieseberg, A. Holzinger, Explainable ai: the new 42?, in: International cross-domain conference for machine learning and knowledge extraction, Springer, 2018, pp. 295–303.
- [10] F. Xu, H. Uszkoreit, Y. Du, W. Fan, D. Zhao, J. Zhu, Explainable ai: A brief survey on history, research areas, approaches and challenges, in: Natural Language Processing and Chinese Computing: 8th CCF International Conference, NLPCC 2019, Dunhuang, China, October 9–14, 2019, Proceedings, Part II 8, Springer, 2019, pp. 563–574.
- [11] C. Molnar, Interpretable machine learning, Lulu. com, 2020.
- [12] I. Tiddi, et al., Foundations of explainable knowledge-enabled systems, *Knowl. Graph. eXplainable Artif. Intell.: Found. Appl. Challenges* 47 (2020) 23.
- [13] F. Lecue, On the role of knowledge graphs in explainable ai, *Semantic Web* 11 (2020) 41–51.
- [14] X.-H. Li, C. C. Cao, Y. Shi, W. Bai, H. Gao, L. Qiu, C. Wang, Y. Gao, S. Zhang, X. Xue, et al., A survey of data-driven and knowledge-aware explainable ai, *IEEE Transactions on Knowledge and Data Engineering* 34 (2020) 29–49.
- [15] Y. Liu, M. Hildebrandt, M. Joblin, M. Ringsquandl, R. Raissouni, V. Tresp, Neural multi-hop reasoning with logical rules on biomedical knowledge graphs, in: The Semantic Web: 18th International Conference, ESWC 2021, Virtual Event, June 6–10, 2021, Proceedings 18, Springer, 2021, pp. 375–391.
- [16] L. Stork, I. Tiddi, R. Spijker, A. ten Teije, Explainable drug repurposing in context via deep reinforcement learning, in: European Semantic Web Conference, Springer, 2023, pp. 3–20.
- [17] E. Ozkan, R. Celebi, A. Yilmaz, V. Emonet, M. Dumontier, Generating knowledge graph based explanations for drug repurposing predictions, in: 14th International Conference on Semantic Web Applications and Tools for Health Care and Life Sciences, 2023, pp. 22–31.
- [18] A. Gottlieb, G. Y. Stein, E. Ruppin, R. Sharan, Predict: a method for inferring novel drug indications with application to personalized medicine, *Molecular systems biology* 7 (2011) 496.
- [19] X. Li, J. F. Rousseau, Y. Ding, M. Song, W. Lu, Understanding drug repurposing from the perspective

- of biomedical entities and their evolution: Bibliographic research using aspirin, *JMIR medical informatics* 8 (2020) e16739.
- [20] M. Nauta, J. Trienes, S. Pathak, E. Nguyen, M. Peters, Y. Schmitt, J. Schlötterer, M. van Keulen, C. Seifert, From anecdotal evidence to quantitative evaluation methods: A systematic review on evaluating explainable ai, *ACM Computing Surveys* 55 (2023) 1–42.
 - [21] G. A. Miller, The magical number seven, plus or minus two: Some limits on our capacity for processing information., *Psychological review* 63 (1956) 81.
 - [22] J. Y. Yen, Finding the k shortest loopless paths in a network, *management Science* 17 (1971) 712–716.
 - [23] E. W. Dijkstra, A note on two problems in connexion with graphs, in: Edsger Wybe Dijkstra: His Life, Work, and Legacy, 2022, pp. 287–290.
 - [24] F. W. Hartel, S. de Coronado, R. Dionne, G. Fragoso, J. Golbeck, Modeling a description logic vocabulary for cancer research, *Journal of biomedical informatics* 38 (2005) 114–129.
 - [25] K. Degtyarenko, P. De Matos, M. Ennis, J. Hastings, M. Zbinden, A. McNaught, R. Alcántara, M. Darsow, M. Guedj, M. Ashburner, Chebi: a database and ontology for chemical entities of biological interest, *Nucleic acids research* 36 (2007) D344–D350.
 - [26] D. S. Himmelstein, A. Lizee, C. Hessler, L. Brueggeman, S. L. Chen, D. Hadley, A. Green, P. Khankhanian, S. E. Baranzini, Systematic integration of biomedical knowledge prioritizes drugs for repurposing, *Elife* 6 (2017) e26726.
 - [27] A. Cormier, M. Knossow, C. Wang, B. Gigant, The binding of vinca domain agents to tubulin: structural and biochemical studies, *Methods in cell biology* 95 (2010) 373–390.